# Nonthermal electron-photon steady states in open cavity quantum materials

**R. Flores-Calderón, Md Mursalin Islam, Michele Pini, Francesco Piazza**

**Angaben zur Veröffentlichung / Publication details:**

Flores-Calderón, R., Md Mursalin Islam, Michele Pini, and Francesco Piazza. 2025. "Nonthermal electron-photon steady states in open cavity quantum materials." Physical Review Research 7 (1): 013073. https://doi.org/10.1103/physrevresearch.7.013073.

# Nonthermal electron-photon steady states in open cavity quantum materials

R. Flores-Calderón [1], Md Mursalin Islam [1], Michele Pini [1], and Francesco Piazza [1,2]
[1] Max Planck Institute for the Physics of Complex Systems, Nöthnitzer Straße 38, 01187 Dresden, Germany
[2] Theoretical Physics III, Center for Electronic Correlations and Magnetism, Institute of Physics, University of Augsburg, 86135 Augsburg, Germany

(Received 17 April 2024; accepted 23 December 2024; published 21 January 2025)

Coupling a system to two different baths can lead to novel phenomena escaping the constraints of thermal equilibrium. In quantum materials inside optical cavities, this feature can be exploited as electrons and cavity photons are easily pulled away from their mutual equilibrium, even in the steady state. This offers new routes for a noninvasive control of material properties and functionalities. We show that the absence of thermal equilibrium between electrons and photons leads to reduced symmetries of the steady-state electronic distribution function. Moreover, by defining an effective temperature from the on-shell distribution function, we find a nonmonotonic behavior as a function of cavity frequency, consistent with recent experimental findings. Finally, we show that, the nonthermal behavior leads to qualitative modifications of the materials properties, as the standard Sommerfeld expansion for observables is modified by a leading-order correction linearly proportional to the temperature difference between the two baths and to the frequency derivative of the electron damping.

DOI: 10.1103/PhysRevResearch.7.013073

## I. INTRODUCTION

Out-of-equilibrium phenomena have resurfaced in multiple areas of physics as a way to circumvent the restrictions imposed by thermal equilibrium. Nonequilibrium steady states, resulting from the coupling of the system of interest to two different baths, are available in various configurations across multiple platforms, ranging from transport in condensed-matter systems, through lasers in atomic and solid-state systems, to active matter and biological systems. In transport for instance two thermal baths act as source and drain of electrons and induce a charge current [1–4]. In active matter such as molecular motors [5–9], the degrees of freedom subject to energy input are different from the ones dissipating it. Similar situations arise in turbulence [10–12], where energy is injected at large length scales and viscously dissipated at short length scales, or in a laser, where electrons inside atoms are externally excited while light is emitted through the mirrors of a cavity [13].

It is in this context that we turn toward cavity quantum materials [14–17], where electrons are coupled on the one hand to the cryostat directly attached to the material, and on the other hand to the discrete set of electromagnetic modes of the cavity, which in turn is coupled through the leaky mirrors to the continuum of electromagnetic modes outside, as schematically shown in Fig. 1. Both the electromagnetic continuum and the cryostat act as thermal baths, but they do not need to be at the same temperature, so that a nonthermal steady state can be achieved. Confining light around quantum materials through cavities has recently emerged as an alternative to the laser-based control [18], with the advantage that weakly, thermally excited electromagnetic fields can be used to affect the material without the large energy input restricting laser-based approaches to pulsed (transient) regimes. In particular, the absence of thermal equilibrium between electrons and photons has been identified as a source of novel phenomenology and enhanced control [19–24].

The present work is particularly motivated by a recent experiment demonstrating cavity control of the metal-to-insulator transition in 1T-$TaS_2$ [24]. The critical temperature associated with the charge-density-wave formation could be substantially modified by tuning only the cavity resonant frequency, despite the light-matter coupling being small relative to the intrinsic electronic scales. So far, the cavity-induced thermal Purcell effect has been suggested as a possible explanation of the large impact in spite of the relatively weak light-matter coupling [24–26], whereby the electrons, due to the cavity environment, experience a temperature different from the one of the cryostat. The experimental observations additionally demand a theoretical explanation for why the critical temperature changes nonmonotonically as a function of the cavity frequency. The proposed explanation based on the Purcell effect is consistent with the nonmonotonic behavior observed experimentally, but is constrained by the assumption of local thermal equilibrium and heat exchange equilibration. Such a condition restricts the magnitude and nature of the predicted effects.

In this work, we propose a scenario where the enhancement of the impact of the cavity on the material and the nonmonotonic behavior as a function of the cavity frequency originate from charge carriers being in a nonthermal steady state. We do not consider the specific charge-density-wave scenario of [24], but rather a simpler model of a two-dimensional metal inside a Fabry-Perot cavity, which makes the generic

nature of the proposed nonthermal mechanism clear. We show that the electronic distribution function reached in the steady-state has a reduced symmetry compared to the thermal equilibrium one, parametrically tuned by the electron-photon coupling, quasiparticle damping, and cavity frequency. From the on-shell nonthermal distribution, a low-energy effective temperature can be extracted from the vicinity of the Fermi surface which behaves nonmonotonically as a function of the cavity frequency, which would explain the nonmonotonic behavior of the critical temperature observed experimentally in Ref. [24]. Moreover, we show that the dominant fluctuation effect on observables is genuinely nonthermal, as the standard Sommerfeld expansion is modified by a correction linearly proportional to the temperature difference between the cavity photons and the cryostat, as well as to the frequency derivative of the electron damping.

While correction to observables which are linear in the temperature difference have been considered before, dating back to Luttinger in 1964 [27], the results we present here do not follow from the these previous works. Indeed, those apply mainly to transport signatures from temperature gradients across the sample, which require a notion of local temperature that we don't have. In our case instead, the coupling of the electrons to the bath and to the photons is homogeneous and as such there is no temperature gradient across the sample. Linear-in-temperature corrections come here from the fact that the two baths to which the electrons are connected with, namely the cryostat and the the cavity-filtered electromagnetic environment, differ not only in temperature but also in their spectral character as well as in the way they couple. We also emphasize that, unlike these previous works, we investigate here the effect on a whole class of observables (Sommerfeld expansion), and we present numerical results also outside of the linear in the $\Delta T$ region.

We finally note that the nonthermal nature of the electronic distribution induced by cavity-photons has been already investigated in terms of its effect on the superconducting gap [19], in analogy to the original Eliashberg effect with oscillating radiofrequency fields [28]. Here, we focus instead on general effects that the cavity-induced nonthermal behavior has on the material's properties.

In Sec. II we present the generic model of a metal cooled by the phonons and the cryostat coupled to cavity photons subject to cavity loss. In Sec. III we present our self-consistent calculation based on Dyson's equation which allows us to obtain a fully quantum kinetic equation for the electron distribution function. Section IV shows the results for the distribution function obtained from the previous approach and highlights how the distribution breaks the thermal symmetry. In Sec. V we calculate an effective temperature both analytically and numerically as a function of the cavity frequency. After this we show how the fermionic distribution modification influences the Sommerfeld expansion for single-particle observables in Sec. VI. Finally, we present our conclusions in Sec. VII.

## II. MODEL

We treat the cavity as two perfectly conducting parallel mirrors with the electrons moving in a plane parallel to the

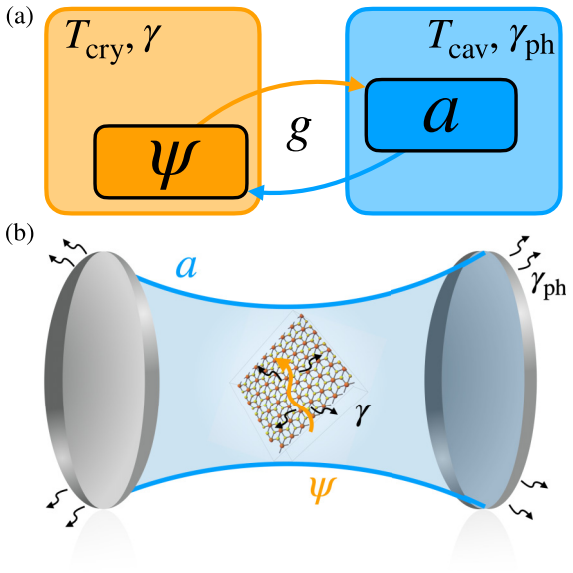


FIG. 1. Schematic representation of the electron-photon system under consideration. (a) Two distinct thermal baths coupled to the electrons (photons) $\psi$ ($a$) and with temperature $T_{\rm cry}$ ($T_{\rm cav}$) and spectral width $\gamma$ ($\gamma_{\rm ph}$) in orange (blue). The electromagnetic field $a$ is coupled to electrons with a strength $g$. (b) Realization with a quantum material within a Fabry-Perot cavity.

mirrors and placed amidst them, as schematically shown in Fig. 1(b). Photons inside the cavity acquire a finite mass because of the boundary conditions, which is set by the cavity fundamental frequency $\nu_0$, appearing in the photon dispersion $\nu_{\mathbf{q}}^2 = \nu_0^2 + c^2\mathbf{q}^2$. For simplicity, we will set $c = 1$ and $\hbar = 1$ throughout the paper. The Hamiltonian for the uncoupled, closed photon-electron system is given by

$$H_0 = \sum_{\mathbf{k}} \epsilon_{\mathbf{k}} \psi_{\mathbf{k}}^\dagger \psi_{\mathbf{k}} + \sum_{\mathbf{q}} \nu_{\mathbf{q}} \left( a_{\mathbf{q}}^\dagger a_{\mathbf{q}} + \frac{1}{2} \right), \tag{1}$$

where the first term models the metallic behavior of the electrons with a gapless dispersion $\epsilon_{\mathbf{k}} = |\mathbf{k}|^2/(2m)$ in $d+1$ space-time dimensions. We have expressed the Hamiltonian in terms of the creation and annihilation operators for the electrons $\{\psi_{\mathbf{k}}, \psi_{\mathbf{k}'}^\dagger\} = \delta_{\mathbf{k},\mathbf{k}'}$, as well as for the cavity photons $[a_{\mathbf{q}}, a_{\mathbf{q}'}^\dagger] = \delta_{\mathbf{q},\mathbf{q}'}$. We couple the electrons to a thermal bath at temperature $T_{\rm cry}$, which physically corresponds to a cryogenically cooled substrate. In the experiment this is given by the cold finger determining the temperature of the material phonons which then act as the thermal bath to the electrons with a Hamiltonian $H_{\text{e-bath}}$. In the Supplemental Material we give an example of the simplest exactly solvable model for a thermal bath, i.e., a bath composed of fermionic degrees of freedom [29]. Using the real-time path-integral formulation on the Keldsyh contour [30,31] we integrate the bath out and the details of such a bath will enter only through the damping rate $\gamma(\mathbf{k}, \omega)$ and temperature $T_{\rm cry}$. Additionally, the leaky cavity mirrors allow the external environmental photons at temperature $T_{\rm cav}$ to act as a thermal bath for the cavity modes. The Hamiltonian for the photon bath and its coupling

to the cavity photons reads

$$H_{\mathrm{ph-bath}} = \sum_{s,\mathbf{q}} \left[ \nu_s(\mathbf{q}) \left( d^\dagger_{s\mathbf{q}} d_{s\mathbf{q}} + \frac{1}{2} \right) + \frac{t^{\mathrm{ph}}_s(\mathbf{q})}{2\sqrt{\nu_{\mathbf{q}}\nu_s(\mathbf{q})}} (a^\dagger_{-\mathbf{q}} + a_{\mathbf{q}})(d^\dagger_{s-\mathbf{q}} + d_{s\mathbf{q}}) \right], \quad (2)$$

where we again consider an extensive number of harmonic oscillators $d_{s\mathbf{q}}$ coupling to each photonic mode of the cavity in a linear fashion. Similarly to the electrons, we integrate out the photon bath within our path-integral formulation to obtain an effective description in terms of the bath temperature $T_{\mathrm{cav}}$ and the resulting photon damping $\gamma_{\mathrm{ph}}(\mathbf{q},\omega) = \sum_s \frac{\pi t^{\mathrm{ph}}_s(\mathbf{q})^2}{4\nu_s(\mathbf{q})} \delta(\omega - \nu_s(\mathbf{q}))$. Finally, we model the electron-photon coupling by a Yukawa-type interaction:

$$V = g \int \mathrm{d}^d \boldsymbol{x}\, \phi(\boldsymbol{x}) \psi^\dagger(\boldsymbol{x}) \psi(\boldsymbol{x}), \quad (3)$$

where $\psi(\boldsymbol{x})$ and $\phi(\boldsymbol{x})$ are the fermionic and real bosonic Fourier transformed operators of $\psi_{\mathbf{k}}$ and $\phi_{\mathbf{q}} = (a_{\mathbf{q}} + a^\dagger_{-\mathbf{q}})/\sqrt{2L\nu_{\mathbf{q}}}$, respectively, $g$ is the light-matter coupling and $L$ is the cavity length. Throughout the rest of the paper, we will set $L$ by its relation with the fundamental cavity frequency $L = \pi/\nu_0$. In Fabry-Perot cavities $g$ is small, typically of the order of 0.1 of the electron bandwidth [16,32,33]. Note that we are using a coupling to the electron density. This might be appropriate for deep-subwavelength cavities [33], but for the Fabry-Perot cavity considered here, a current coupling should actually be used. We argue however that the qualitative nonequilibrium features of the system can be highlighted also with the simpler density coupling of Eq. (3). For the sake of simplicity, we also consider a momentum-independent coupling $g$. The total Hamiltonian we consider is thus $H = H_0 + H_{\mathrm{e-bath}} + H_{\mathrm{ph-bath}} + V$.

## III. DYSON EQUATION APPROACH

Our goal is to compute the electron distribution function $F(\mathbf{k},\omega)$ in the steady state of the open system. We cannot assume thermal equilibrium, plus electrons and photons cannot in principle be treated classically. Therefore, a classical (Langevin or Fokker-Planck) approach is not suitable, while a standard Boltzmann-type equation for the electrons is restricted to the case of a small electron-bath coupling ensuring well-defined quasiparticles [19]. We thus choose to start with coupled Dyson equations for the electron's and photon's distribution functions. Since we are dealing with an interacting system—the electron-photon coupling is not linear—we adopt a self-consistent one-loop approach [34,35] which can be obtained within the real-time path-integral formulation illustrated in the Supplemental Material [29]. We proceed now by neglecting the back action of the electrons onto the photons, which is valid as long as the photon-bath coupling, quantified by $\gamma_{\mathrm{ph}}$, is sufficiently larger than the coupling $g$. Further assuming space- and time-translation invariance in the steady state, the resulting equation for the electron distribution function reads

$$\gamma(\mathbf{k},\omega)\Delta F(\mathbf{k},\omega) = g^2 \sum_{\mathbf{k}'} \int_{\tilde{\omega}} A(\mathbf{k}',\tilde{\omega}) A_{\mathrm{ph}}(\mathbf{k}'-\mathbf{k},\tilde{\omega}-\omega) \times \{B_0(\tilde{\omega}-\omega)[F(\mathbf{k}',\tilde{\omega}) - F(\mathbf{k},\omega)] - 1 + F(\mathbf{k},\omega)F(\mathbf{k}',\tilde{\omega})\}, \quad (4)$$

where $\int_{\tilde{\omega}} \equiv \int \frac{\mathrm{d}\tilde{\omega}}{2\pi}$, and we have defined the deviation of the distribution function from equilibrium $\Delta F(\mathbf{k},\omega) = F(\mathbf{k},\omega) - F_0(\omega)$, along with the thermal distribution functions for the electrons $F_0(\omega) = \tanh[(\omega-\mu_0)/(2T_{\mathrm{cry}})]$ and the photons $B_0(\omega) = \coth[\omega/(2T_{\mathrm{cav}})]$. We have introduced here the electron chemical potential or Fermi energy $\mu_0$ set by the bath. We have also written the right hand side in terms of the spectral functions of the electrons $A(\mathbf{k},\omega)$ and the photons $A_{\mathrm{ph}}(\mathbf{k},\omega)$, which are defined as $A(\mathbf{k},\omega) = \frac{\gamma(\mathbf{k},\omega)}{(\omega-\epsilon_{\mathbf{k}})^2+\gamma^2(\mathbf{k},\omega)}$ and $A_{\mathrm{ph}}(\mathbf{q},\omega) = \frac{\nu_0}{\pi} \frac{\gamma_{\mathrm{ph}}(\omega)}{(\omega^2-\nu^2_{\mathbf{q}})^2+\gamma^2_{\mathrm{ph}}(\omega)}$. Within the simple model introduced above, the quasiparticle dampings $\gamma$ and $\gamma_{\mathrm{ph}}$ are set by the baths.

If the photon damping, setting the width of the spectral function, it will be sufficiently smaller than the electron damping, $\gamma_{\mathrm{ph}} \ll \gamma$, as well as the temperatures, $\gamma_{\mathrm{ph}} \ll T_{\mathrm{cry}}, T_{\mathrm{cav}}$. We can treat the photon spectral function $A_{\mathrm{ph}}(\mathbf{k},\omega)$ as a Dirac-delta peaked at the photon dispersion to perform the frequency integral in Eq. (4). Furthermore, the momentum integral can be similarly performed by observing that the photons in the cavity have an extremely light mass compared to the electronic effective mass coming from the dispersion relation in typical solid-state materials. This allows to treat the momentum dependence of the photon spectral function also as a delta function at zero momentum. As shown in the Supplemental Material [29], performing these approximations leads to a self-consistent equation for the distribution function of the form

$$\Delta F(\mathbf{k},\omega) = \frac{g^2}{4\pi\gamma(\mathbf{k},\omega)} [A(\mathbf{k},\omega+\nu_0)H_{\nu_0}(\mathbf{k},\omega) - A(\mathbf{k},\omega-\nu_0)H_{-\nu_0}(\mathbf{k},\omega)], \quad (5)$$

where we defined $H_\nu(\mathbf{k},\omega) = B_0(\nu)[F(\mathbf{k},\omega+\nu) - F(\mathbf{k},\omega)] + F(\mathbf{k},\omega)F(\mathbf{k},\omega+\nu) - 1$. Let us consider the following two regimes: $\nu_0 \ll T_{\mathrm{cav}}, T_{\mathrm{cry}}, \gamma$ or $\nu_0 \gg T_{\mathrm{cav}}, T_{\mathrm{cry}}, \gamma$. In the Supplemental Material [29], we show that, at the lowest order in both regimes, one finds $F(\mathbf{k},\omega) = F_0(\omega)$. Moreover, in the small $\nu_0$ limit, Eq. (5) can be expanded to the linear order in $\nu_0$ and assumes the form of a nonlinear differential equation, for which a further analytic treatment is possible. Given a $g$ which is much smaller than the electronic energy scales, we can perform a weak coupling expansion of the nonlinear differential equation (see the Supplemental Material [29]), which results in the leading order correction for the distribution:

$$\Delta F = \frac{g^2\nu_0\Delta T\gamma(\mathbf{k},\omega)}{4\pi T_{\mathrm{cry}} A(\mathbf{k},\omega)} \frac{\partial}{\partial\omega} \left[ \frac{A(\mathbf{k},\omega)}{\gamma(\mathbf{k},\omega)} \operatorname{sech}\left( \frac{\omega-\mu_0}{2T_{\mathrm{cry}}} \right) \right]^2, \quad (6)$$

where the temperature difference is defined as $\Delta T = T_{\mathrm{cav}} - T_{\mathrm{cry}}$. In this case, the out of equilibrium contribution is proportional to the temperature difference between the two

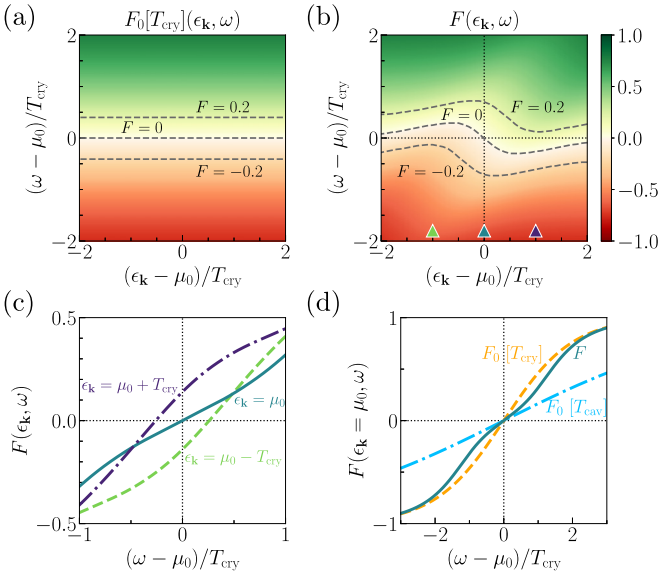


FIG. 2. Distribution function from the numerical solution of Eq. (5). (a) Noninteracting thermal solution $F_0(\omega)$ at the cryostat temperature $T_{\rm cry}$. This is antisymmetric around the line $\omega=\mu_0$. (b) Nonthermal distribution $F(\mathbf{k},\omega)$ with fixed $T_{\rm cav}/T_{\rm cry}=3$, $\nu_0/T_{\rm cry}=0.5$, $\gamma_0/T_{\rm cry}=0.5$, $\mu_0/T_{\rm cry}=100$, and $g/T_{\rm cry}=1$. Note that it has anti-inversion symmetry about the point $(\epsilon_{\mathbf{k}}=\mu_0,\omega=\mu_0)$. (c) Nonthermal distribution cuts for different momentum values (fixed through $\epsilon_{\mathbf{k}}$), corresponding to the colored triangles in panel (b). (d) Comparison of the thermal distributions $F_0[T](\omega)=\tanh[(\omega-\mu_0)/(2T)]$ at $T=T_{\rm cry}$, $T_{\rm cav}$ and the nonthermal $F(\mathbf{k},\omega)$ at the Fermi momentum $(\epsilon_{\mathbf{k}}=\mu_0)$.

baths, thus $\Delta T$ amplifies the photon-induced redistribution. In Eq. (6) we observe an explicit momentum dependence of the nonthermal distribution, which is absent in the thermal distribution $F_0(\omega)$. Moreover, we see that the nonthermal deviation $\Delta F(\mathbf{k},\omega)$ is parametrically tuned by the coupling $g$, the quasiparticle damping $\gamma(\mathbf{k},\omega)$, and the cavity frequency $\nu_0$. As we will show later, this analytical solution is also able to capture the leading-order behavior of the on-shell effective temperature for small $\nu_0$ and $g$.

## IV. BROKEN THERMAL SYMMETRY AND STEADY-STATE DISTRIBUTION FUNCTION

We turn now to discuss the full solution obtained iteratively from Eq. (5). We focus here on the simple case of a momentum and frequency-independent electron dissipation $\gamma_0=\gamma(\mathbf{k},\omega)$, and we show the corresponding $F(\mathbf{k},\omega)$ in Fig. 2. Note that, for a dissipation $\gamma_0$, the momentum dependence of $F(\mathbf{k},\omega)$ enters only through $\epsilon_{\mathbf{k}}$. The nonthermal nature of the distribution becomes clearly visible when comparing the upper two panels. Thermal symmetry for $g\to 0$ [36] implies that in the $(\epsilon_{\mathbf{k}},\omega)$ plane we have an inversion antisymmetry along the $\omega=\mu_0$ line given by $F_0(\mu_0+\chi)=-F_0(\mu_0-\chi)$, as shown in Fig. 2(a). For finite coupling, the distribution function develops a momentum dependence and the antisymmetry around $\omega=\mu_0$ is broken. Instead, the distribution has now an antisymmetry around the inversion point $(\epsilon_{\mathbf{k}},\omega)=(\mu_0,\mu_0)$ given by $F(\mu_0+\xi,\mu_0+\chi)=-F(\mu_0-\xi,\mu_0-\chi)$, as easily seen in the contours shown in Fig. 2(b).

The role of a nonzero $\gamma$ is indeed fundamental, already from the QKE it can be shown that if the right hand side vanishes, the resulting distribution is purely thermal with temperature $T_{\rm cav}$. The addition of a nonzero damping rate thus acts as a relaxation mechanism allowing the electrons to reach a nonthermal steady state with a different symmetry than the usual thermal one. We effectively have a driven-dissipative system with two unequal sources and sinks. This imbalance leads to a loss of detailed balance and an inherent broken thermal symmetry. The resulting reduced symmetry in the distribution function would then depend strongly on the functional form of the damping rate. Indeed, from Eq. (6) we observe that keeping the frequency dependence of the damping $\gamma(\omega)$ will remove also the inversion antisymmetry around the point $(\mu_0,\mu_0)$.

Furthermore, the frequency dependence of the distribution is shown in Fig. 2(c), at fixed values of $\epsilon_{\mathbf{k}}$, away from the Fermi momentum $(\epsilon_{\mathbf{k}}\neq\mu_0)$, the zero crossing of $F$ is shifted from the origin, indicating a nonthermal nature. Even for the distribution at the Fermi momentum $(\epsilon_{\mathbf{k}}=\mu_0)$, we see a nonthermal interpolation of $F(\mu_0,\omega)$ between the distribution at the cavity temperature around the Fermi energy $\omega\approx\mu_0$ and the distribution at the cryostat temperature at large frequencies, as depicted in Fig. 2(d). It is worth noting that these results are not substantially changed by considering a finite photon damping rate. Indeed, the overall discussion and calculations are based on the hierarchy of scales which ensures that $\gamma_{\rm ph}$ is much smaller than the bath temperatures and the electron damping rate but still bigger than the smallest energy scale coming from the coupling $g$. Within these assumptions, the final expressions are independent of $\gamma_{\rm ph}$. Moreover, even when $\gamma_{\rm ph}$ does not respect this hierarchy, the results remain qualitatively the same, i.e., the distribution has the same reduced symmetry and nonthermal behavior, as shown in the Supplemental Material [29].

## V. EFFECTIVE ON-SHELL TEMPERATURE IN THE NONTHERMAL STEADY STATE

Although the electron distribution is nonthermal, it is useful to look at its low-energy properties near the Fermi surface. Like in the previous section, we simplify our treatment and assume $\gamma(\mathbf{k},\omega)=\gamma_0$. We can extract an effective temperature $T_{\rm eff}^{\text{on-shell}}$ from the on-shell nonthermal distribution $F(\mathbf{k},\omega=\epsilon_{\mathbf{k}})$ by linearizing it around $\epsilon_{\mathbf{k}}\simeq\mu_0$, meaning $T_{\rm eff}^{\text{on-shell}}=\frac{1}{2}\left[\frac{\partial F(\mathbf{k},\epsilon_{\mathbf{k}})}{\partial\epsilon_{\mathbf{k}}}\right]^{-1}_{\epsilon_{\mathbf{k}}=\mu_0}$. We find for small $\nu_0$ and $g$,

$$T_{\rm eff}^{\text{on-shell}}=(1-\alpha)^{-1}T_{\rm cry},\quad \alpha=\frac{g^2\nu_0\Delta T}{4\pi\gamma_0^2T_{\rm cry}^2}. \tag{7}$$

In a similar spirit to the thermal Purcell effect [24,25], we can thus observe that the effective electron temperature depends on the cavity geometry, which enters in our model through the cavity frequency $\nu_0$. We remark however that here, in contrast to the thermal Purcell picture, the electrons are in a nonthermal distribution $F(\mathbf{k},\omega)$, and the effective temperature $T_{\rm eff}^{\text{on-shell}}$ represents only a local property of the on-shell distribution function around $\epsilon_{\mathbf{k}}\simeq\mu_0$. The effective

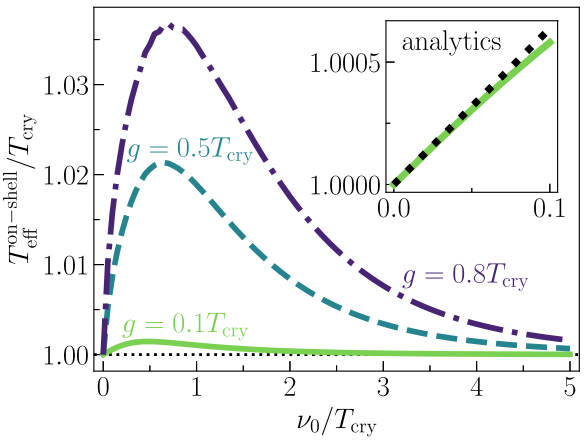


FIG. 3. Effective on-shell temperature $T_{\rm eff}^{\rm on\text{-}shell} = \frac{1}{2}[\frac{\partial F(\mathbf{k},\epsilon_\mathbf{k})}{\partial \epsilon_\mathbf{k}}]^{-1}_{\epsilon_\mathbf{k}=\mu_0}$ calculated from the numerical solution of Eq. (5) vs cavity frequency $\nu_0$, for three values of the coupling $g$ and with parameters $T_{\rm cav}/T_{\rm cry} = 3$, $\mu_0/T_{\rm cry} = 100$, and $\gamma_0/T_{\rm cry} = 0.5$. The inset shows the agreement of the full numerical solution (green solid line) with the analytical solution for small $\nu_0$ and $g$ in Eq. (7).

temperature $T_{\rm eff}^{\rm on\text{-}shell}$ is shown in Fig. 3. Interestingly, from the numerical solution we observe a nonmonotonic dependence of the $T_{\rm eff}^{\rm on\text{-}shell}$ on $\nu_0$. Whenever the physics of a phase transition is governed by the vicinity of the Fermi surface, we can thus predict a nonmonotonic behavior of any critical temperature measured in terms of the cryostat temperature $T_{\rm cry}$, as it is observed in the experiment [24].

## VI. NONTHERMAL SOMMERFELD EXPANSION

In a noninteracting Fermi gas at thermal equilibrium, the expectation values of a single-particle observable $\hat{O} = \int dt \sum_\mathbf{k} o_\mathbf{k}(t)\psi^\dagger_\mathbf{k}(t)\psi_\mathbf{k}(t)$ at low temperature can be expressed as a power series of the temperature $T$ by means of the Sommerfeld expansion [37]. Due to the antisymmetry property of the equilibrium distribution $F_0(\omega)$ around $\omega = \mu_0$, the leading order temperature-dependent term is always quadratic in temperature and linear in the energy derivative of the observable $(\pi^2T^2/6)\partial_\epsilon[O(\epsilon)D(\epsilon)]_{\epsilon=\mu_0}$, where $O(\epsilon_\mathbf{k}) = o_\mathbf{k}(\omega = \epsilon_\mathbf{k})$ and $D(\epsilon)$ is the density of states. We describe how this picture is modified in our two-bath setting for time-independent single-particle observables, taking into account the frequency dependence of the quasiparticle damping $\gamma(\omega)$ [38]. In a setting with a finite electron damping, one also needs to define the frequency-integrated distribution $\tilde{F}(\epsilon) = \int \frac{d\omega}{\pi} A(\mathbf{k},\omega)F(\epsilon,\omega)$, [in the standard case [37] one typically has $\gamma \to 0$, which corresponds to $\tilde{F}(\epsilon) = F(\epsilon, \omega = \epsilon)$]. To obtain a closed expression for this correction, we consider $\langle\hat{O}\rangle = \int \mathrm{d}\epsilon\, O(\epsilon)\, D(\epsilon)\tilde{f}(\epsilon)$, where we defined $\tilde{f} = (1 - \tilde{F})/2$. We assume that the width $\gamma(\omega = \mu_0)$ of the spectral function is much smaller than the chemical potential $\mu_0$, and we further assume that $T_{\rm cry} \ll \mu_0$, as per the usual Sommerfeld expansion. In the limits of small $\nu_0$ and small $g$, we can use the analytical solution (6) for the nonthermal distribution, and obtain the following change (see the Supplemental Material for details of the derivation [29]):

$$\Delta\langle\hat{O}\rangle \equiv \int \mathrm{d}\epsilon\; O(\epsilon)\, D(\epsilon)[\tilde{f}(\epsilon) - \tilde{f}_0(\epsilon)]$$
$$= \frac{g^2\nu_0\Delta T}{4\pi\gamma_0^3} O(\mu_0)D(\mu_0)\partial_\omega\gamma(\omega)|_{\omega=\mu_0}. \qquad (8)$$

We see that this new term is linear in the temperature difference $\Delta T = T_{\rm cav} - T_{\rm cry}$ and also proportional to the value of the observable evaluated at the chemical potential. It is also linearly proportional to the frequency derivative of the electron damping. For a generic thermal bath, such as the phonons to which the electrons couple once the cold finger is placed, the damping rate can have a nontrivial frequency dependence and thus we expect an important contribution from Eq. (8). Moreover, even for a frequency independent $\gamma$, we still find a similar modification in the expectation value of time dependent observables, where now we have the result:

$$\Delta\langle\hat{O}\rangle = \frac{g^2\nu_0\Delta T}{4\pi\gamma_0^2} D(\mu_0)O'(\omega)\Big|_{\omega=\mu_0}. \qquad (9)$$

This term shows again the fundamental nonthermal linear-in-temperature-difference behavior and the characteristic $g$, $\nu_0$ dependence. A term like (8) or (9) is prohibited at thermal equilibrium due to the antisymmetry of $\tilde{F}(\epsilon)$ around $\epsilon = \mu_0$ excluding odd powers of $T_{\rm cry}$ from the expansion.

## VII. CONCLUSIONS

We have studied nonthermal electron steady states in open cavity quantum materials. Furthermore, we defined an effective temperature from the behavior of the nonthermal on-shell distribution function near the Fermi surface, and have shown that it depends nonmonotonically on the cavity frequency, which is consistent with the nonmonotonic behavior of critical temperature of the charge-density-wave transition observed in the experiment of Ref. [24]. In future work, we will extend our investigation of the effects of the nonthermal electron distribution function to the critical temperature and gap equation. Moreover, we have shown that, in the Sommerfeld expansion of a single-particle observable, a nonthermal correction appears, which is proportional to the temperature difference between the two baths, to the observable evaluated at the Fermi surface, as well as to the frequency derivative of the electron damping. The findings highlight the importance of taking into account nonthermal effects in two-bath settings through the modified fermionic distribution function, and how this generically can induce qualitative changes in the material's properties.

## ACKNOWLEDGMENT

We thank Martin Eckstein, Daniele Fausti, Denis Golez, and Zala Lenarcic for fruitful discussions.

[1] K. von Klitzing, T. Chakraborty, P. Kim, V. Madhavan, X. Dai, J. McIver, Y. Tokura, L. Savary, D. Smirnova, A. M. Rey, C. Felser, J. Gooth, and X. Qi, 40 years of the quantum Hall effect, Nat. Rev. Phys. **2**, 397 (2020).

[2] R. J. J. Mackenbach, J. H. E. Proll, and P. Helander, Available energy of trapped electrons and its relation to turbulent transport, Phys. Rev. Lett. **128**, 175001 (2022).

[3] L. Ren, L. Lombez, C. Robert, D. Beret, D. Lagarde, B. Urbaszek, P. Renucci, T. Taniguchi, K. Watanabe, S. A. Crooker, and X. Marie, Optical detection of long electron spin transport lengths in a monolayer semiconductor, Phys. Rev. Lett. **129**, 027402 (2022).

[4] S. Ryu and H.-S. Sim, Partition of two interacting electrons by a potential barrier, Phys. Rev. Lett. **129**, 166801 (2022).

[5] D. Needleman and Z. Dogic, Active matter at the interface between materials science and cell biology, Nat. Rev. Mater. **2**, 17048 (2017).

[6] G. Popkin, The physics of life, Nature (London) **529**, 16 (2016).

[7] W. Xi, T. B. Saw, D. Delacour, C. T. Lim, and B. Ladoux, Material approaches to active tissue mechanics, Nat. Rev. Mater. **4**, 23 (2019).

[8] M. Foglino, E. Locatelli, C. A. Brackley, D. Michieletto, C. N. Likos, and D. Marenduzzo, Non-equilibrium effects of molecular motors on polymers, Soft Matter **15**, 5995 (2019).

[9] G. Pacchioni, Molecular motors: You spin me round, Nat. Rev. Mater. **1**, 16045 (2016).

[10] Y. Pomeau, The long and winding road, Nat. Phys. **12**, 198 (2016).

[11] G. Lemoult, L. Shi, K. Avila, S. V. Jalikop, M. Avila, and B. Hof, Directed percolation phase transition to sustained turbulence in Couette flow, Nat. Phys. **12**, 254 (2016).

[12] M. Oberlack, S. Hoyas, S. V. Kraheberger, F. Alcántara-Ávila, and J. Laux, Turbulence statistics of arbitrary moments of wall-bounded shear flows: A symmetry approach, Phys. Rev. Lett. **128**, 024502 (2022).

[13] A. E. Siegman, *Lasers* (University Science Books, California, 1986).

[14] F. J. Garcia-Vidal, C. Ciuti, and T. W. Ebbesen, Manipulating matter by strong coupling to vacuum fields, Science **373**, eabd0336 (2021).

[15] F. Mivehvar, F. Piazza, T. Donner, and H. Ritsch, Cavity qed with quantum gases: New paradigms in many-body physics, Adv. Phys. **70**, 1 (2021).

[16] F. Schlawin, D. M. Kennes, and M. A. Sentef, Cavity quantum materials, Appl. Phys. Rev. **9**, 011312 (2022).

[17] J. Bloch, A. Cavalleri, V. Galitski, M. Hafezi, and A. Rubio, Strongly correlated electron–photon systems, Nature (London) **606**, 41 (2022).

[18] A. de la Torre, D. M. Kennes, M. Claassen, S. Gerber, J. W. McIver, and M. A. Sentef, *Colloquium*: Nonthermal pathways to ultrafast control in quantum materials, Rev. Mod. Phys. **93**, 041002 (2021).

[19] J. B. Curtis, Z. M. Raines, A. A. Allocca, M. Hafezi, and V. M. Galitski, Cavity quantum Eliashberg enhancement of superconductivity, Phys. Rev. Lett. **122**, 167002 (2019).

[20] A. Chakraborty and F. Piazza, Long-range photon fluctuations enhance photon-mediated electron pairing and superconductivity, Phys. Rev. Lett. **127**, 177002 (2021).

[21] A. Chakraborty and F. Piazza, Controlling collective phenomena by engineering the quantum state of force carriers: The case of photon-mediated superconductivity and its criticality, arXiv:2207.07131.

[22] C. J. Eckhardt, S. Chattopadhyay, D. M. Kennes, E. A. Demler, M. A. Sentef, and M. H. Michael, Theory of resonantly enhanced photo-induced superconductivity, Nat. Commun. **15**, 2300 (2024).

[23] E. Viñas Boström, A. Sriram, M. Claassen, and A. Rubio, Controlling the magnetic state of the proximate quantum spin liquid $\alpha$-$RuCl_3$ with an optical cavity, npj Comput. Mater. **9**, 202 (2023).

[24] G. Jarc, S. Y. Mathengattil, A. Montanaro, F. Giusti, E. M. Rigoni, R. Sergo, F. Fassioli, S. Winnerl, S. Dal Zilio, D. Mihailovic *et al.*, Cavity-mediated thermal control of metal-to-insulator transition in $1T - TaS_2$, Nature (London) **622**, 487 (2023).

[25] G. Chiriacò, Thermal purcell effect and cavity-induced renormalization of dissipations, Phys. Rev. B **110**, L161107 (2023).

[26] F. Fassioli, J. Faist, M. Eckstein, and D. Fausti, Controlling radiative heat flow through cavity electrodynamics, arXiv:2403.00851.

[27] J. M. Luttinger, Theory of thermal transport coefficients, Phys. Rev. **135**, A1505 (1964).

[28] G. Eliashberg, Film superconductivity stimulated by a high-frequency field, Technical Report, Institute of Theoretical Physics, Moscow, 1970.

[29] See Supplemental Material at http://link.aps.org/supplemental/10.1103/PhysRevResearch.7.013073 for detailed calculation for the electron distribution function in the steady state using the Keldysh formalism, additionally we calculate the modified Sommerfeld expansion.

[30] A. Kamenev, *Field theory of non-equilibrium systems* (Cambridge University Press, 2023).

[31] L. M. Sieberer, M. Buchhold, and S. Diehl, Keldysh field theory for driven open quantum systems, Rep. Prog. Phys. **79**, 096001 (2016).

[32] F. Schlawin, A. Cavalleri, and D. Jaksch, Cavity-mediated electron-photon superconductivity, Phys. Rev. Lett. **122**, 133602 (2019).

[33] G. M. Andolina, A. De Pasquale, F. M. D. Pellegrino, I. Torre, F. H. L. Koppens, and M. Polini, Amperean superconductivity cannot be induced by deep subwavelength cavities in a two-dimensional material, Phys. Rev. B **109**, 104513 (2024).

[34] F. Piazza and P. Strack, Quantum kinetics of ultracold fermions coupled to an optical resonator, Phys. Rev. A **90**, 043823 (2014).

[35] P. Rao and F. Piazza, Non-fermi-liquid behavior from cavity electromagnetic vacuum fluctuations at the superradiant transition, Phys. Rev. Lett. **130**, 083603 (2023).

[36] In the Supplemental Material we prove that for $g \to \infty$ the solution is the Fermi-Dirac distribution with the photon-bath temperature $T_{\text{cav}}$. In the opposite limit $g \to 0$, the right hand side in Eq. (5) vanishes, such that the solution becomes $F(\mathbf{k}, \omega) = F_0(\omega)$, which is trivially expected for a vanishing coupling to the photons.

[37] N. W. Ashcroft and N. D. Mermin, *Solid State Physics* (Holt-Saunders, 1976).

[38] For time-dependent observables, a constant electron damping $\gamma(\omega) = \gamma_0$ can generate a nonthermal correction, as shown in the Supplemental Material.